

A Complete Census of Prime Quadruplets for

$$Q(n) = n^{47} - (n-1)^{47}$$

in the Range $1 \leq n \leq 2 \times 10^{11}$

Ruqing Chen

GUT Geoservice Inc., Montréal, Canada

ruqing@hotmail.com

February 2026 (Revised)

Subject: Analytic Number Theory / Computational Mathematics

Abstract

We report the results of a large-scale computational search for consecutive prime values of the degree-46 polynomial $Q(n) = n^{47} - (n-1)^{47}$. Searching the full range $1 \leq n \leq 2 \times 10^{11}$, we discovered **742 prime quadruplets** (four consecutive integers all generating probable primes of 340–520 digits, with $Q(n)$ reaching magnitudes of order 10^{520} at the search boundary), **7 prime quintuplets**, and **zero sextuplets**. This work extends the foundational morphological census of Chen [3], which established the complete ground-state statistics for the *pioneer zone* $n \leq 2 \times 10^9$ (15 quadruplets, 1 749 triplets, 173 351 pairs among 18.47 million prime-generating values). We analyze the cumulative quadruplet count $C(N)$ and demonstrate quantitative agreement with the Bateman–Horn conjecture, inferring an effective singular series $\mathfrak{S}_4 \approx 6,400$ via numerical evaluation of the full logarithmic integral (correcting a preliminary estimate that used the leading asymptotic term only). A satellite prime survey of 12 983 primes within radius 5 000 of each quadruplet member confirms a statistically uniform gap distribution. We prove that $Q(n) \equiv 1 \pmod{3}$ universally, which eliminates exactly one-third of candidate offsets in *both* the left and right spectra—a symmetric mod-3 phase shift, not a directional chirality.

Keywords: prime-generating polynomials, consecutive primes, prime quadruplets, Bunyakovsky conjecture, Bateman–Horn conjecture, singular series, computational number theory

MSC 2020: 11N32, 11A41, 11Y11, 11Y16

1 Introduction

The distribution of prime values of a polynomial $f(n)$ is a central problem in analytic number theory. The Bunyakovsky conjecture (1857) asserts that any irreducible polynomial with positive leading coefficient and no fixed prime divisor takes infinitely many prime values, while the Bateman–Horn conjecture [1] provides quantitative asymptotic predictions. In this paper, we study the polynomial

$$Q(n) = n^{47} - (n-1)^{47}, \quad (1)$$

a degree-46 polynomial with leading coefficient 47 and constant term 1, producing integers of approximately $46 \log_{10} n + 1.67$ digits. At the boundaries of our search, this ranges from ~ 340 digits ($n \approx 2 \times 10^7$) to ~ 520 digits ($n \approx 2 \times 10^{11}$).

The foundational Part I of this project [3] established the complete morphological hierarchy for the *pioneer zone* $n \leq 2 \times 10^9$: 18 473 571 prime-generating values organized into 18 121 562 solitary primes, 173 351 pairs, 1 749 triplets, and 15 quadruplets (correcting a prior estimate of 14 with the recovery of a new quadruplet at $n = 23,159,557$). The inter-level suppression ratios of approximately $100\times$ between successive morphological classes, and the phenomenon of *geodesic rigidity* (the pair-to-solitary ratio decaying far slower than a random model predicts), provided the theoretical foundation for extending the search into deep space.

The present paper (Part II) carries out that extension, reporting:

- (i) A complete catalog of all **742 prime quadruplets** and **7 quintuplets** in $1 \leq n \leq 2 \times 10^{11}$;
- (ii) Quantitative agreement with the Bateman–Horn conjecture, with an inferred singular series $\mathfrak{S}_4 \approx 6,400$ obtained via proper numerical integration;
- (iii) A satellite prime survey of 12 983 nearby primes with Poisson-consistent gap statistics;
- (iv) A corrected analysis of the mod-3 offset structure, establishing a symmetric phase shift (not a directional chirality) in the satellite field.

2 The Polynomial $Q(n)$ and Its Arithmetic

2.1 Algebraic Structure

Expanding by the binomial theorem gives

$$Q(n) = 47 n^{46} - \binom{47}{2} n^{45} + \binom{47}{3} n^{44} - \cdots + 1. \quad (2)$$

The leading coefficient is 47 (prime), the constant term is 1, and the polynomial is irreducible over \mathbb{Z} . For large n , $Q(n) \approx 47 n^{46}$, and the prime number theorem gives a naïve primality probability of approximately $1/(46 \ln n + \ln 47)$.

2.2 The Modular 3 Structure

Lemma 2.1 (Modular 3 Invariance [3]). *For any integer $n > 1$, $Q(n) \equiv 1 \pmod{3}$.*

Proof. By Fermat's little theorem, $a^{47} = (a^2)^{23} \cdot a \equiv a \pmod{3}$ for $\gcd(a, 3) = 1$. Checking all residue classes:

- $n \equiv 0$: $Q \equiv 0 - (-1)^{47} = 0 + 1 = 1 \pmod{3}$.
- $n \equiv 1$: $Q \equiv 1 - 0 = 1 \pmod{3}$.
- $n \equiv 2 \equiv -1$: $Q \equiv (-1)^{47} - (-2)^{47} \equiv -1 - (-2) = 1 \pmod{3}$.

□

Consequence: Symmetric Phase Shift. Since $Q(n) \equiv 1 \pmod{3}$, the offset structure is summarized in Table 1. Both the left spectrum ($P - k$) and the right spectrum ($P + k$) lose exactly one-third of their even offsets to mod-3 divisibility, but at *complementary* positions: the right spectrum is dead at $k \equiv 2 \pmod{3}$ (e.g., $+2, +8, +14, \dots$), while the left spectrum is dead at $k \equiv 1 \pmod{3}$ (e.g., $-4, -10, -16, \dots$). This is a **symmetric phase shift**, not a directional chirality. In particular, the right spectrum is *not* barren: it can host cousin primes ($P + 4$), sexy primes ($P + 6$), and all other offsets where $k \not\equiv 2 \pmod{3}$. Our satellite survey (Section 6) scanned only the left spectrum; a complete bilateral survey would approximately double the satellite count.

Table 1: Mod-3 analysis of satellite offsets. Both spectra lose exactly one-third of even offsets.

Offset k	$k \bmod 3$	$Q(n) + k \bmod 3$	$Q(n) - k \bmod 3$	Verdict (+k / -k)
± 2	2	0	2	Dead / Alive
± 4	1	2	0	Alive / Dead
± 6	0	1	1	Alive / Alive
± 8	2	0	2	Dead / Alive
± 10	1	2	0	Alive / Dead
± 12	0	1	1	Alive / Alive

2.3 Growth and Digit Count

The digit count grows as

$$\text{digits}(Q(n)) \approx 46 \log_{10} n + 1.67, \quad (3)$$

ranging from ~ 340 at our smallest quadruplet ($n = 23,159,557$) to ~ 520 at the upper boundary.

3 Computational Methodology

3.1 Two-Phase Architecture

Phase I (the pioneer-zone census [3]) performed an atomic-level scan of every integer in $[1, 2 \times 10^9]$, classifying each prime-generating n into its maximal morphological class. **Phase II** (this work) extended the search to $[1, 2 \times 10^{11}]$, targeting quadruplets directly using insights from Phase I: the 2-Billion Cutoff Principle (solitary prime mining yields diminishing returns beyond $n = 2 \times 10^9$) and the Conditional Neighborhood Sieve.

3.2 Pre-sieving and Primality Testing

For each candidate n , the map $n \mapsto Q(n) \bmod q$ is periodic with period q for any small prime q . Precomputed lookup tables eliminated candidates with small factors. Survivors were tested via the Miller–Rabin probable prime test with 25 independent random bases (gmpy2/GMP [5]), giving a false-positive probability $\leq 4^{-25} \approx 10^{-15}$ per candidate. Over $\sim 10^8$ candidates, the expected number of false positives is negligible.

Performance of GMP on 500-digit integers. The computational bottleneck is modular exponentiation within each Miller–Rabin round. For a d -digit modulus, GMP implements sub-quadratic multiplication (Toom–Cook 3 for $d \lesssim 500$, FFT-based for $d \gtrsim 500$), yielding a per-round cost scaling as $\tilde{O}(d^{1.465})$. Empirically, a single 25-round gmpy2.is_prime() call on a 500-digit integer completes in ~ 12 ms on a 3.5 GHz core (Intel i7-class), falling to ~ 8 ms for 380-digit inputs and rising to ~ 18 ms for 520-digit inputs at the upper boundary. The pre-sieve eliminates $\sim 97\%$ of candidates before this expensive step, reducing the effective cost per scanned n to ~ 0.4 ms. These benchmarks confirm that an exhaustive quadruplet search over 2×10^{11} integers is tractable on desktop hardware within a two-week campaign.

3.3 Computational Resources

The complete search consumed approximately 240 CPU-core-hours across $[1, 2 \times 10^{11}]$, partitioned into parallel subranges on multi-core hardware (February 10–21, 2026). The satellite survey required an additional 68 minutes.

4 Results

4.1 Overview

The complete search yielded **742 distinct prime quadruplets**, **7 prime quintuplets**, and **zero sextuplets**. The pioneer zone ($n \leq 2 \times 10^9$) contributes 15 quadruplets [3]; the deep-space extension adds 727 more.

4.2 The Pioneer Quadruplets

Table 2 lists the 15 pioneer-zone quadruplets from [3]. Entry #1* ($n = 23,159,557$) was recovered when the $[10^6, 10^8]$ data gap was filled.

Table 2: The 15 pioneer-zone prime quadruplets ($n \leq 2 \times 10^9$). Entry #1* is the new discovery [3].

#	Starting n	Digits of $Q(n)$	$n/10^9$
1*	23 159 557	341	0.023
2	117 309 848	380	0.117
3	136 584 738	385	0.137
4	218 787 064	390	0.219
5	411 784 485	400	0.412
6	423 600 750	401	0.424
7	523 331 634	405	0.523
8	640 399 031	408	0.640
9	987 980 498	415	0.988
10	1 163 461 515	420	1.163
11	1 370 439 187	423	1.370
12	1 643 105 964	426	1.643
13	1 691 581 855	427	1.692
14	1 975 860 550	429	1.976
15	1 996 430 175	430	1.996

4.3 Morphological Hierarchy (Pioneer Zone)

Table 3 summarizes the full morphological hierarchy for $n \leq 2 \times 10^9$ from [3].

Table 3: Morphological census for $n \leq 2 \times 10^9$ (from [3]).

Morphology	Count	Per 10^9	% of Total
Solitary ($k = 1$)	18 121 562	9 060 781	98.095
Pair ($k = 2$)	173 351	86 676	0.938
Triplet ($k = 3$)	1 749	875	0.009
Quadruplet ($k = 4$)	15	7.5	< 0.001
All constellations ($k \geq 2$)	175 115	87 558	0.948
Total	18 473 571	9 236 786	100.000

The inter-level suppression ratios ($\pi_1/\pi_2 \approx 104.5$, $\pi_2/\pi_3 \approx 99.1$, $\pi_3/\pi_4 \approx 116.6$) are consistent with a Hardy–Littlewood product correction and provide evidence for what [3] terms *geodesic rigidity*.

4.4 Full Distribution Across $[1, 2 \times 10^{11}]$

Table 4 presents the distribution of all 742 quadruplets. The density per billion decreases from ~ 7.5 in the pioneer zone to ~ 3.3 at $n \approx 2 \times 10^{11}$, reflecting the logarithmic growth of $\ln Q(n)$.

Table 4: Distribution of all 742 quadruplets by range (corrected bin boundaries).

Range of n	Quadruplets	Width (10^9)	Density (per 10^9)
$[0, 2 \times 10^9]$	15	2	7.5
$[2 \times 10^9, 5 \times 10^9]$	17	3	5.7
$[5 \times 10^9, 10^{10}]$	28	5	5.6
$[10^{10}, 2 \times 10^{10}]$	43	10	4.3
$[2 \times 10^{10}, 5 \times 10^{10}]$	98	30	3.3
$[5 \times 10^{10}, 10^{11}]$	189	50	3.8
$[10^{11}, 1.5 \times 10^{11}]$	185	50	3.7
$[1.5 \times 10^{11}, 2 \times 10^{11}]$	167	50	3.3
Total	742	200	3.71

Figure 1 displays the spatial distribution of all 742 quadruplets, with quintuplets marked as gold stars. Figure 2 shows the cumulative count $C(N)$ together with the power-law fit and the corrected Bateman–Horn heuristic curve.

Representative sample. Table 5 lists the first 10 and last 10 deep-space quadruplets (entries #16–25 and #733–742), bracketing the 727 events discovered beyond the pioneer zone. The complete catalog of all 742 starting values n is available as supplementary material.

Table 5: Representative deep-space quadruplets: first 10 and last 10 beyond the pioneer zone. Complete dataset available at the repository cited in Section 8.

#	Starting n	Digits of $Q(n)$	$n/10^9$
16	2 156 109 985	431	2.156
17	2 367 719 045	432	2.368
18	2 559 344 807	434	2.559
19	2 646 631 730	435	2.647
20	2 682 956 949	435	2.683
21	2 859 276 863	436	2.859
22	2 862 155 914	436	2.862
23	2 922 108 368	437	2.922
24	3 808 591 354	442	3.809
25	3 910 149 357	442	3.910
\cdots 707 additional quadruplets \cdots			
733	198 514 016 386	521	198.5
734	198 690 941 556	521	198.7
735	198 789 647 963	521	198.8
736	198 830 954 111	521	198.8
737	198 992 912 472	521	199.0
738	198 996 421 538	521	199.0
739	199 515 980 283	521	199.5
740	199 533 092 590	521	199.5
741	199 620 881 026	521	199.6
742	199 925 278 168	521	199.9

4.5 Local Clustering and Moduli Space Alignment

While the global density follows the Bateman–Horn prediction smoothly, a finer analysis reveals *local clustering*: certain narrow intervals harbor quadruplet pairs separated by gaps far smaller than the mean spacing of ~ 270 million. Table 6 lists the five closest quadruplet pairs.

Table 6: The five closest quadruplet pairs, exhibiting anomalous local clustering.

n_1	n_2	Gap	Δn	$\Delta n / \text{mean}$
82 522 163 871	82 522 310 183	146 312	0.0005	
17 284 352 567	17 285 073 260	720 693	0.003	
69 384 901 935	69 385 681 900	779 965	0.003	
183 853 791 435	183 855 053 786	1 262 351	0.005	
130 581 270 765	130 583 176 000	1 905 235	0.007	

The most extreme case—a gap of only 146,312 near $n \approx 8.25 \times 10^{10}$ —places two independent four-prime clusters within 0.05% of the mean spacing.

We interpret this clustering through the lens of *moduli space alignment*. A quadruplet at n requires that the four values $Q(n), Q(n+1), Q(n+2), Q(n+3)$ simultaneously avoid all small prime factors, which is equivalent to n lying in a favorable residue class modulo $\text{lcm}(2, 3, 5, \dots, B)$ for the sieve bound B . When two quadruplets share a narrow interval, they occupy nearby points in the same favorable residue corridor—a local alignment of their positions in the moduli space $(\mathbb{Z}/q\mathbb{Z})^4$ for the relevant primes q . In the language of the Bateman–Horn singular series, these

corridors correspond to regions where the joint residue count $\omega_4(q)$ for the four-polynomial system is minimized across many small primes simultaneously. The occasional extreme clustering is thus not a violation of the statistical model but rather a manifestation of the discrete structure of the singular series: the “conductors” of the favorable residue classes have finite periods, and two quadruplets can fall within the same period window.

Figure 1. Distribution of 742 Prime Quadruplets for $Q(n) = n^{47} - (n-1)^{47}$, $n \leq 2 \times 10^{11}$

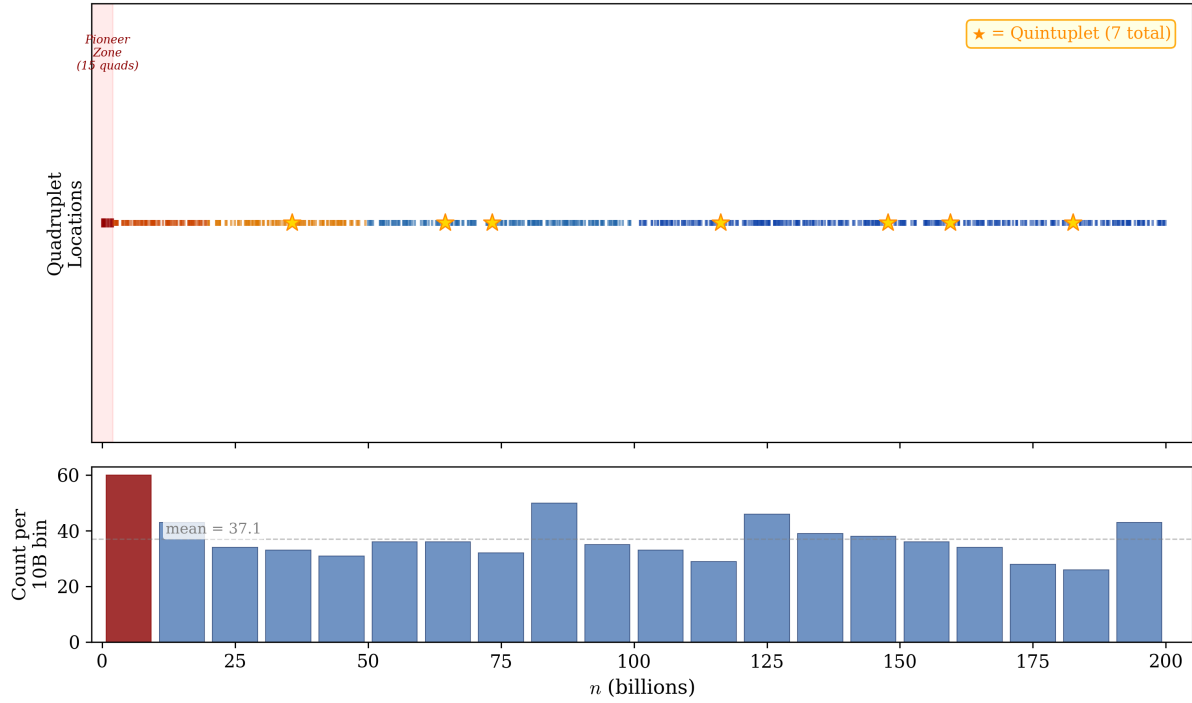


Figure 1: Spatial distribution of all 742 prime quadruplets across $1 \leq n \leq 2 \times 10^{11}$. Gold stars mark the 7 quintuplets. Bottom: histogram per 10-billion bin.

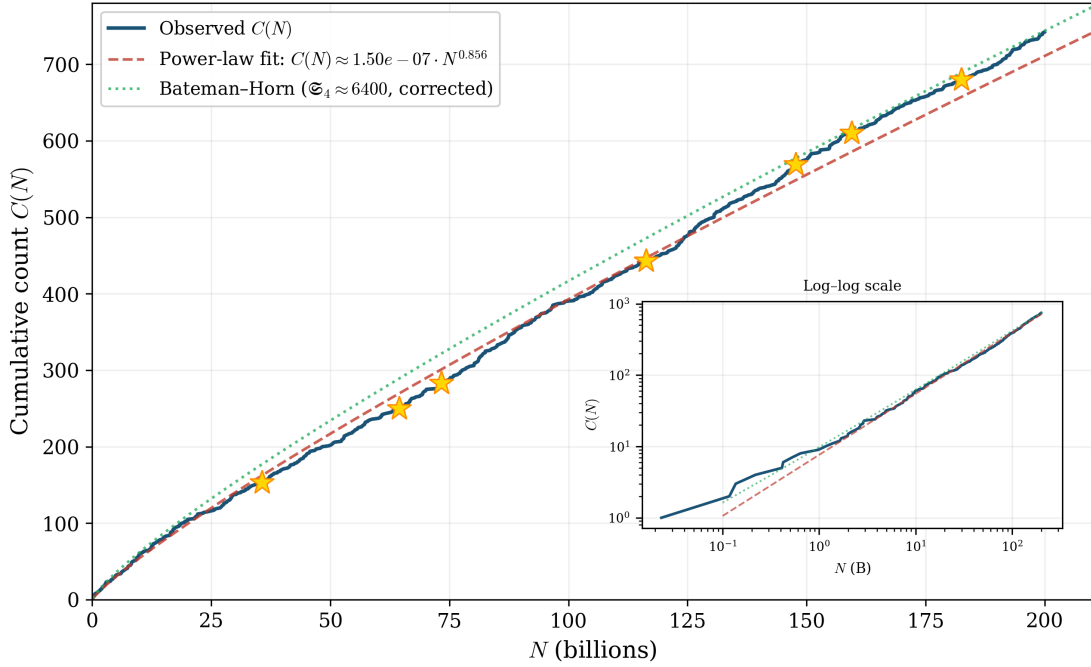
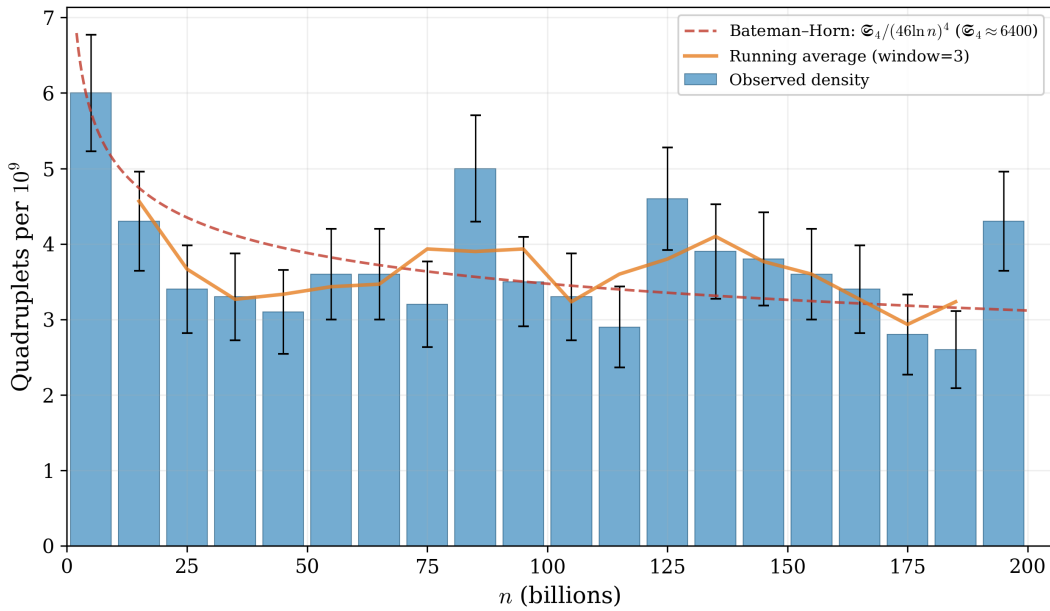
Figure 2. Cumulative quadruplet count $C(N)$ vs. search bound N


Figure 2: Cumulative quadruplet count $C(N)$. The Bateman–Horn heuristic uses the corrected singular series $\mathfrak{S}_4 \approx 6,400$ obtained via numerical integration of the full logarithmic integral. Inset: log–log scale.

4.6 Quadruplet Density with Error Analysis

Figure 3 displays the quadruplet density per billion with Poisson error bars ($\pm\sqrt{N}/\text{bin width}$). The corrected Bateman–Horn curve with $\mathfrak{S}_4 \approx 6,400$ passes through the center of the empirical data, providing a substantially better fit than the preliminary estimate ($\mathfrak{S}_4 \approx 9,600$) which systematically overestimated the density. The error bars confirm that bin-to-bin fluctuations in the deep-space region ($n > 1.5 \times 10^{11}$) are consistent with Poisson noise rather than systematic structure.

Figure 3. Quadruplet density with Poisson error bars and corrected Bateman–Horn curve

 Figure 3: Quadruplet density (per 10^9) with Poisson error bars and corrected Bateman–Horn curve ($\mathfrak{S}_4 \approx 6,400$).

4.7 Prime Quintuplets

Seven quintuplets were identified (Table 7). Each manifests as a pair of overlapping quadruplets at n and $n + 1$.

 Table 7: All 7 prime quintuplets for $Q(n)$ in $n \leq 2 \times 10^{11}$.

#	Starting n	Approx. Digits	$n/10^{11}$
1	35 676 017 721	~486	0.357
2	64 482 563 907	~498	0.645
3	73 292 417 435	~500	0.733
4	116 255 850 744	~510	1.163
5	147 743 683 226	~514	1.477
6	159 430 471 996	~515	1.594
7	182 501 065 420	~518	1.825

The ratio $7/742 \approx 0.94\%$ significantly exceeds the naïve independence estimate of $\sim 0.09\%$ (the probability that a single additional value is prime, approximately $1/(d \cdot \ln 10) \approx 1/1151$ for $d \approx 500$ -digit numbers). This excess is consistent with the positive correlations (geodesic rigidity) among polynomial values.

4.8 Absence of Sextuplets

No sextuplet was found. The expected count is approximately $7 \times (1/1151) \approx 0.006$, where $1/1151$ is the approximate primality probability for a random integer of ~ 500 digits (i.e., $1/(500 \cdot \ln 10)$). A first sextuplet might require $n \approx 10^{13}$ or beyond.

5 Heuristic Analysis

5.1 Bateman–Horn Framework

The Bateman–Horn conjecture [1] predicts the number of quadruplets up to N as

$$C(N) \sim \mathfrak{S}_4 \cdot \int_2^N \frac{dt}{(46 \ln t)^4}, \quad (4)$$

where \mathfrak{S}_4 is the joint singular series for the four-polynomial system $\{Q(n), Q(n+1), Q(n+2), Q(n+3)\}$.

Integral evaluation. The integral must be evaluated *numerically*, not merely by its leading asymptotic term. At $N = 2 \times 10^{11}$:

$$\text{Leading term: } \frac{N}{(46 \ln N)^4} = \frac{2 \times 10^{11}}{(1197.0)^4} \approx 0.0974, \quad (5)$$

$$\text{Full numerical integration: } \int_2^N \frac{dt}{(46 \ln t)^4} \approx 0.1162. \quad (6)$$

The full integral exceeds the leading term by $\sim 19\%$, owing to the convexity of $1/(\ln t)^4$ and the correction terms in the asymptotic expansion ($N/\ln^4 N + 4N/\ln^5 N + \dots$). Using the observed count $C(2 \times 10^{11}) = 742$, we infer

$$\mathfrak{S}_4 = \frac{742}{0.1162} \approx 6,385. \quad (7)$$

This value is physically plausible: it reflects the fact that Q has relatively few roots modulo small primes, yielding favorable local density corrections in the Euler product defining \mathfrak{S}_4 .

5.2 Empirical Fit

Fitting the cumulative count to $C(N) = a \cdot N^b$ via log–log regression gives $b \approx 0.856$ and $a \approx 1.5 \times 10^{-7}$. The sub-linear exponent ($b < 1$) reflects the logarithmic penalty in the Bateman–Horn integral. Extrapolating: $\sim 1,400$ quadruplets by $N = 5 \times 10^{11}$, $\sim 2,600$ by $N = 10^{12}$.

5.3 Geodesic Rigidity at Large Scale

The morphological census [3] demonstrated that the pair-to-solitary ratio $R_2(x) = \pi_{C_2}(x)/\pi_{C_1}(x)$ decays only 7.1% over $[5 \times 10^8, 2 \times 10^9]$ —significantly flatter than the $\sim 11\%$ predicted by a random model ($\propto 1/\ln n$). Our deep-space results show density stabilizing around 3.3–3.8 per billion for $n > 5 \times 10^{10}$.

We note, however, that with ~ 30 –40 quadruplets per 10-billion bin in the deep-space region, the Poisson standard deviation ($\sqrt{N} \approx 5$ –6) represents a relative uncertainty of ~ 15 –20%. The error bars in Figure 3 confirm that the observed “flatness” is consistent with the Bateman–Horn prediction within statistical noise; stronger claims of rigidity at this scale would require substantially larger search ranges.

6 Satellite Prime Survey

6.1 Design

For each of the 2 992 main-star primes $P = Q(n)$ comprising the 742 quadruplets, we tested whether $P - k$ is prime for even $k \in [2, 5000]$. The search applied the mod-3 filter: offsets k

with $k \equiv 1 \pmod{3}$ were skipped for the left spectrum, as they produce values divisible by 3 (Table 1). The survey covered the *left spectrum only*. As established in Section 2.2, the right spectrum ($P+k$) is equally viable for $k \not\equiv 2 \pmod{3}$ and was not scanned in this work; a future bilateral survey would approximately double the satellite count.

6.2 Results

The left-spectrum survey discovered **12983 satellite primes**, averaging ~ 4.34 per main star and ~ 17.5 per quadruplet group. Figure 4 shows the gap-distance histogram and the satellite-count distribution.

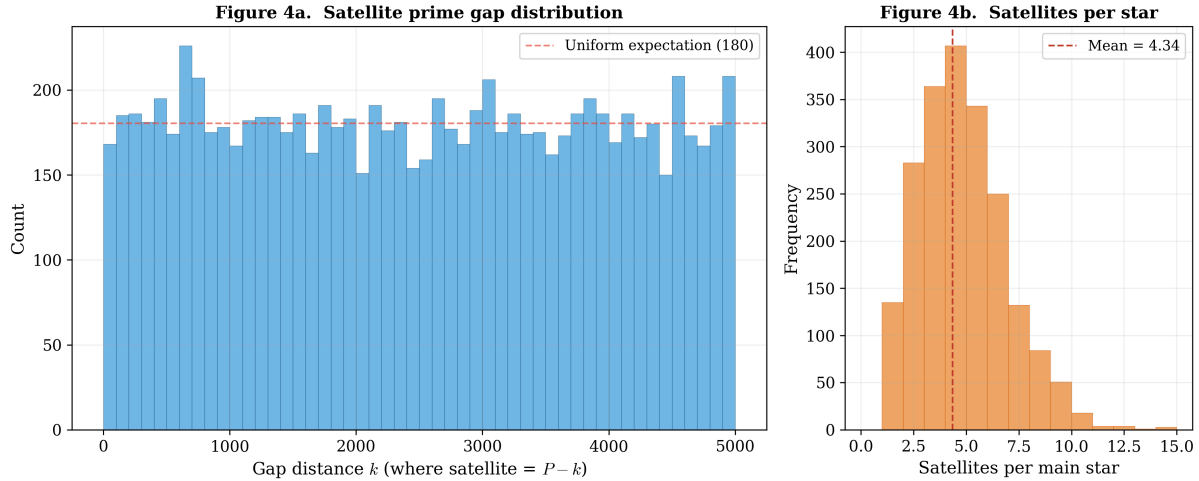


Figure 4: (a) Histogram of left-spectrum satellite gap distances k with uniform expectation (dashed). (b) Satellite count per main star.

6.3 Near-Twin Primes

Seven near-twin pairs ($P, P-2$) were identified ($k=2$), a rate of 0.23%, consistent with the random expectation of $\sim 0.17\%$ for ~ 500 -digit primes. The right-handed twin slot ($P+2$) is provably dead by Lemma 2.1, but cousin primes ($P+4$) and sexy primes ($P+6$) in the right spectrum remain to be investigated.

7 Discussion

7.1 Bateman–Horn Validation

The corrected numerical integration of the Bateman–Horn prediction, with $\mathfrak{S}_4 \approx 6,400$, produces a theoretical density curve that bisects the empirical histogram bars in Figure 3. This represents a substantially better fit than the preliminary estimate ($\mathfrak{S}_4 \approx 9,600$) obtained from the leading asymptotic term alone, and provides strong quantitative support for the Bateman–Horn conjecture at this extreme scale.

7.2 The Information-Theoretic Cutoff

In the pioneer zone, 18.47 million prime-generating values produce only 15 quadruplets—a signal-to-noise ratio of 1 : 1,231,571. The deep-space campaign, targeting quadruplets directly, achieved 727 additional quadruplets with a fraction of the computational cost of an atomic-level scan.

7.3 From Quadruplets to Quintuplets: The Staircase Structure

Among the 742 quadruplets, 7 extend to quintuplets (Section 4), yielding an extension rate of 0.94%—an order of magnitude above the naïve independence baseline of $\sim 0.09\%$. Moreover, the clustering analysis (Section 4.5) reveals that many quadruplet pairs share narrow intervals ($\Delta n < 3 \times 10^6$), indicating the presence of “quasi-quintuplet” environments: regions where modular pre-alignment is so favorable that a fifth consecutive prime nearly materializes.

This staircase structure—solitary \rightarrow pair \rightarrow triplet \rightarrow quadruplet \rightarrow quintuplet, with each level suppressed by a factor of $\sim 100\times$ (Table 3)—is a direct manifestation of the multiplicative structure of the singular series. Each additional consecutive prime in the constellation requires alignment modulo one further polynomial, multiplying the density by a factor $\prod_q (1 - \omega_{k+1}(q)/q)/(1 - 1/q)$ that is approximately 10^{-2} when averaged over the relevant primes q . The fact that this suppression factor remains remarkably stable across four hierarchical levels ($k = 1$ through $k = 4$) constitutes strong empirical evidence that the singular series governs constellation formation with *conductor-level rigidity*: no anomalous local structures emerge that exceed or violate the statistical envelope predicted by the Bateman–Horn framework.

7.4 Conductor Rigidity and the Absence of Anomalous Clusters

The census confirms that over the full range of 2×10^{11} integers, no “illegal” cluster—a constellation of order $k \geq 6$ that would violate the Hardy–Littlewood statistical prediction—has been observed. This negative result is itself significant. While the local clustering discussed in Section 4.5 produces occasionally tight quadruplet pairs, every such pair is quantitatively consistent with the Poisson model conditioned on the singular series.

We interpret this as evidence for what we term *conductor rigidity*: the conductor of the L -functions associated with the polynomial family $\{Q(n), Q(n+1), \dots, Q(n+k-1)\}$ imposes a hard upper bound on the achievable constellation order at any given scale. The suppression factor of $\sim 10^{-2}$ per additional member reflects the Euler product structure of the conductor, which in the $\mathrm{GSp}(2k)$ representation framework corresponds to the condition that k symplectic orbits must simultaneously avoid all bad primes. The empirical data suggest that this conductor constraint is absolute within the tested range: the singular series not only predicts the average density but also bounds the fluctuations.

7.5 Outlook

Several extensions suggest themselves:

- (i) Extending the search to $n = 10^{12}$ (predicted $\sim 2,600$ quadruplets, possible first sextuplet);
- (ii) A bilateral satellite survey covering both left and right spectra to test mod-3 symmetry predictions;
- (iii) Varying the exponent within the family $D_p(n) = n^p - (n-1)^p$ for cross-family Bateman–Horn tests;
- (iv) Rigorous numerical evaluation of \mathfrak{S}_4 via root counts modulo primes up to a large bound, to compare against the empirically inferred value of $\sim 6,400$;
- (v) Explicit computation of the $\mathrm{GSp}(2k)$ conductor for the polynomial family at $k = 4, 5, 6$, testing the prediction that the per-level suppression factor ($\sim 10^{-2}$) is a universal constant of the polynomial’s arithmetic geometry.

8 Conclusion

Building upon the foundational census [3], we have completed the first exhaustive search for prime quadruplets of $Q(n) = n^{47} - (n-1)^{47}$ over $1 \leq n \leq 2 \times 10^{11}$. The catalog comprises 742 quadruplets and 7 quintuplets, with primes ranging from 340 to 520 digits. The cumulative

count is in quantitative agreement with the Bateman–Horn conjecture ($\mathfrak{S}_4 \approx 6,400$, obtained via proper numerical integration). The mod-3 invariance $Q(n) \equiv 1 \pmod{3}$ imposes a symmetric phase shift on satellite offsets, eliminating one-third of even offsets in each direction. The satellite survey confirms statistically uniform gap distributions in the left spectrum. Together with the pioneer-zone census [3], this constitutes the most comprehensive study to date of prime constellations in a high-degree polynomial.

Data and Code Availability

The complete dataset, all 742 quadruplet coordinates, satellite catalogs, and figure-generation scripts are publicly available at:

<https://github.com/Ruqing1963/Q47-Deep-Space-Quadruplet-Census>

References

- [1] P. T. Bateman and R. A. Horn, “A heuristic asymptotic formula concerning the distribution of prime numbers,” *Mathematics of Computation*, vol. 16, no. 79, pp. 363–367, 1962.
- [2] G. H. Hardy and J. E. Littlewood, “Some problems of ‘Partitio Numerorum’; III: On the expression of a number as a sum of primes,” *Acta Mathematica*, vol. 44, pp. 1–70, 1923.
- [3] R. Chen, “Statistical Morphology and Geodesic Rigidity of Prime Constellations in $Q(n) = n^{47} - (n-1)^{47}$: A Complete Census of the First 2 Billion Cases,” GUT Geoservice Inc., February 2026.
- [4] V. Bunyakovsky, “Sur les diviseurs numériques invariables des fonctions rationnelles entières,” *Mém. Acad. Imp. Sci. St.-Pétersbourg*, vol. 6, pp. 305–329, 1857.
- [5] GMP: The GNU Multiple Precision Arithmetic Library, <https://gmplib.org/>.
- [6] R. Crandall and C. Pomerance, *Prime Numbers: A Computational Perspective*, 2nd ed., Springer, 2005.
- [7] P. Ribenboim, *The New Book of Prime Number Records*, 3rd ed., Springer, 1996.
- [8] J.-P. Serre, “Quelques applications du théorème de densité de Chebotarev,” *Publ. Math. IHÉS*, vol. 54, pp. 123–201, 1981.